JOURNAL OF COLLOID AND INTERFACE SCIENCE 157, 100–112 (1993)

Lateral Capillary Forces between Floating Submillimeter Particles

V. N. PAUNOV,* P. A. KRALCHEVSKY,†,[1] N. D. DENKOV,*,[2] AND K. NAGAYAMA†

* *Laboratory of Thermodynamics and Physico-chemical Hydrodynamics, University of Sofia, Faculty of Chemistry, Sofia 1126, Bulgaria; and † Protein Array Project, ERATO, JRDC, 18-1 Higashiarai, Tsukuba 305, Japan*

Received May 22, 1992; accepted September 10, 1992

A procedure for calculating the energy and force of capillary interaction between two floating spherical particles of submillimeter size attached to a liquid–fluid interface is proposed on the basis of a general expression for the grand thermodynamic potential of the system. The latter takes into account the gravitational, wetting, and meniscus surface energies. For large interparticle separations the derived equations reduce to the asymptotic formulas derived by Chan *et al.* (*J. Colloid Interface Sci.* 79, 410 (1981)). The effects of interfacial tension, particle size, density, and contact angle on the capillary interaction are investigated. The results of the energetical and force approaches to the capillary interactions turn out to be in a very good quantitative agreement.

1. INTRODUCTION

The capillary interactions between small particles floating attached to a liquid–fluid interface were observed long ago and utilized in some extraction and separation techniques—see e.g. Refs. (1, 2). When the particles are similar, the capillary forces are attractive and lead to formation of two-dimensional aggregates at the liquid surface. These forces were studied experimentally by Hinsch (3) and Camoin *et al.* (4).

The main theoretical problem with the capillary forces is to solve the Laplace equation of capillarity, which in general is a second-order nonlinear partial differential equation, which determines the profile of the liquid meniscus around the particles. A numerical approach was developed by Gifford and Scriven (5) for the case of two identical infinite parallel horizontal cylinders, when the meniscus has translational symmetry. Nicolson (6) derived an approximate analytic expression for the capillary force between two floating bubbles. He used a superposition approximation: the meniscus profile is a superposition of the profiles around two single bubbles, each of them having rotational symmetry. This approach is applicable when the meniscus slope is small and the Laplace equation can be linearized. In addition, the interparticle separation should be large compared with the particle size in order that the boundary conditions at the three-phase contact lines (the Neumann–Young equation) be satisfied. A considerable development of Nicolson's approach was achieved by Chan *et al.* (7), who derived theoretical expressions for the energy and force of capillary interaction in the case of floating spheres and horizontal cylinders. These expressions hold for not-too-small interparticle separations because of the usage of the superposition approximation. An alternative approach was proposed by Fortes (8).

A recent development in the theory of capillary meniscus interactions is based on an asymptotic solution of the Laplace equation in bipolar coordinates in the cases of two identical particles (9), two different particles (10), and particle–wall interaction (11). More precisely, Refs. (9–11) investigate the capillary forces between vertical cylinders and/or spherical particles, which are partially immersed in a liquid layer on a horizontal substrate; i.e., the vertical movement of the particles is restricted by the presence of the solid substrate. One should note that in the latter case the weight of the particles does not affect the capillary forces.

The aim of the present paper is to apply the approach developed in Refs. (9, 10) for studying the capillary forces between spherical particles floating attached to a liquid–fluid interface, when the meniscus deformations are due to the particle weight. This approach can lead to an improvement of the previous study of the same subject, Ref. (7), in the following two aspects: (i) The usage of bipolar coordinates in Refs. (9, 10) enables one to impose the exact boundary conditions (the Neumann–Young equations) at the two contact lines and to calculate their elevation even for interparticle separations comparable with the particle radius, when the capillary forces are stronger; (ii) In the approach of Nicolson, used in Ref. (7), it is assumed that the energy of capillary interaction between floating particles coincides with the particle gravitational potential energy. The validity of this assumption will be verified below in comparison with the general approach proposed in Ref. (9), which takes into account not only the gravitational energy of the particles and of the two neighboring fluid phases, but also the changes in the wetting and meniscus surface energies due to meniscus deformation under the particle weight.

[1] On temporary leave from the University of Sofia, Bulgaria.

[2] To whom correspondence should be addressed.

0021-9797/93 $5.00

In the next section the geometry of the system under consideration is described. A general expression for the energy of capillary interaction is derived in Section 3. This expression is specified in Section 4 by using the balance of forces acting on a particle. In Section 5 the available equations for calculating the elevations of the contact lines are discussed. Asymptotic expressions for the capillary forces are derived and discussed in Section 6. The calculation procedure is described in Section 7. Finally, the numerical results are presented and discussed.

2. CONFIGURATION OF THE INTERFACES

Let us consider the capillary meniscus around two spherical particles of radii R_1 and R_2 floating at a liquid–fluid interface—see Fig. 1. Each of the particles protrudes from the lower phase, and three-phase contact lines of radii r_1 and r_2 are formed. α_1 and α_2 are the respective contact angles at which the fluid interface meets the particle surfaces. Far from the particles, the interface is flat and horizontal. The coordinate plane xy is chosen to coincide with the plane of the horizontal interface. The plane xz is vertical and passes through the particle centers.

We denote by $\zeta(x, y)$ the function describing the shape of the meniscus surface. The explicit form of $\zeta(x, y)$ can be determined by solving the Laplace equation of capillarity—see Section 5 below. The values of ζ can be positive in the case of light particles (Fig. 1a) and negative in the case of heavy particles (Fig. 1b). h_k and ψ_k, $k = 1, 2$, shown in Fig. 1 characterize the meniscus elevation and slope at the respective contact line. More precisely, the two contact lines are not perfectly horizontal (the deviation from horizontality is very small for $qR_k < 1$—see Ref. (7); q^{-1} is the capillary length—see below). That is why we consider h_k as being the mean elevation of the contact line

$$h_k = \frac{1}{2\pi r_k} \oint_{C_k} \zeta_k(l)\,dl, \quad k = 1, 2, \qquad [2.1]$$

where C_k is a contour representing the projection of the contact line on the horizontal plane xy and $z = \zeta_k(l)$ represents the equation of the contact line. As shown in Figs. 1a and 1b, h_k and ψ_k are positive for light particles and negative for heavy particles.

The parameter b_k ($k = 1, 2$) shown in Figs. 1a and 1b characterizes the depth of immersion of the respective particle inside the lower fluid (phase I). Thus for the z-coordinate of the sphere center one obtains

$$Z_k^{(c)} = h_k - b_k + R_k, \quad k = 1, 2. \qquad [2.2]$$

The volume of the part of the sphere which is immersed into the lower phase is

$$V_l^{(k)} = \pi b_k^2 (R_k - b_k/3), \quad k = 1, 2, \qquad [2.3]$$

supposing that the contact line is horizontal. The radius of the contact line is also a function of b_k:

$$r_k = [b_k(2R_k - b_k)]^{1/2}, \quad k = 1, 2. \qquad [2.4]$$

The above expressions will be used below to calculate the capillary interaction energy.

3. CAPILLARY INTERACTION ENERGY

Our aim here is to determine the capillary interaction energy of two particles floating attached to the interface between phases I and II of mass densities ρ_I and ρ_{II}, respectively. The surface tension of this phase boundary will be denoted by γ. The quantity $q^{-1} = [\gamma/(\rho_I - \rho_{II})g]^{1/2}$, with g being the gravity acceleration, is the capillary length, characterizing the range of the capillary interactions—see below. We will follow the general approach developed in Ref. (9). According to Eq. [2.2] in Ref. (9) the free energy of the system can be represented as a superposition of gravitational, wetting, and liquid meniscus contributions:

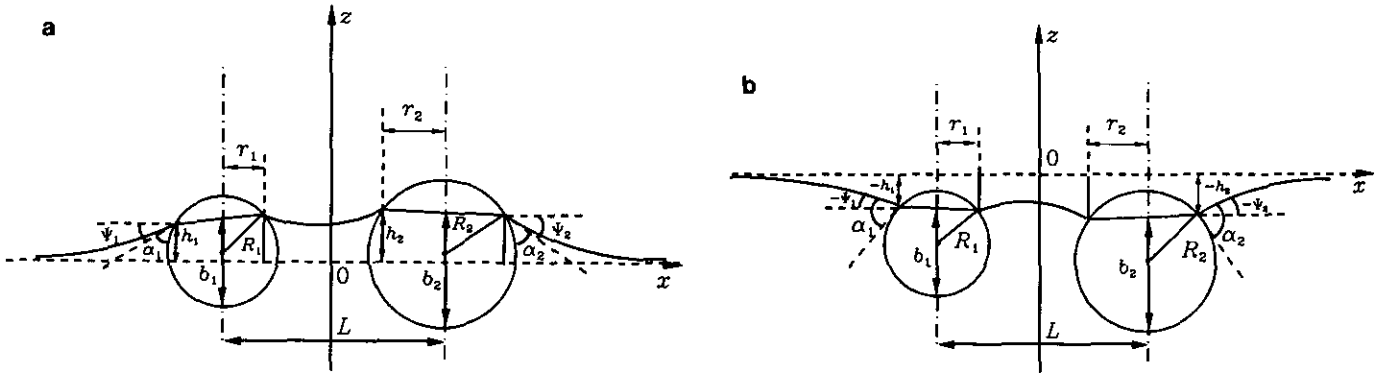

FIG. 1. Sketch of the capillary meniscus around two spherical particles of radii R_1 and R_2 at a distance L in the case of (a) light and (b) heavy particles. α_1 and α_2 are the three-phase contact angles and r_1 and r_2 are the radii of the contact lines.

$$W = W_g + W_w + W_m. \quad [3.1]$$

The term

$$W_g = \sum_{k=1}^{2} m_k g Z_k^{(c)} + \sum_{Y=I,II} m_Y g Z_Y^{(c)} \quad [3.2]$$

accounts for the gravitational energy of the particles and phases I and II, respectively, whose masses are denoted by m_k and m_Y; $Z_k^{(c)}$ and $Z_Y^{(c)}$ represent the z-coordinates of the respective particle or phase mass centers:

$$V_k Z_k^{(c)} = \int_{V_k} z dV \quad \text{and} \quad V_Y Z_Y^{(c)} = \int_{V_Y} z dV;$$

$$(k = 1, 2; Y = I, II). \quad [3.3]$$

To ensure the convergence of the integral over V_Y we suppose that the system under consideration, depicted in Fig. 1, is closed in a container of a very large (compared with the capillary length) but still finite size. The exact choice of this container is not important for the final results, because the capillary interaction energy is an excess quantity—see Eq. [3.6] below.

The surface free energy of the particles is

$$W_w = \sum_{k=1}^{2} \sum_{Y=I,II} \omega_{kY} A_{kY}, \quad [3.4]$$

with A_{kY} being the area of the interface between the particle k and the phase Y, and ω_{kY} being the respective surface free energy density. The last term in Eq. [3.1],

$$W_m = \gamma \Delta A, \quad [3.5]$$

represents the free surface energy of the liquid meniscus (the interface between phases I and II); ΔA is defined as the difference between the areas of the meniscus surface and its orthogonal projection on the plane xy—see Fig. 1.

Since the free energy, W, is defined with respect to an arbitrary additive constant, it is convenient to choose the reference zero state to be the free energy of the same particles, taken at infinite (very large compared with the capillary length) interparticle separation, W_∞. Then the interaction energy, ΔW, between particles 1 and 2 can be defined by

$$\Delta W = W - W_\infty. \quad [3.6]$$

As shown in Ref. (10), the contribution of the meniscus surface energy, ΔW_m, to the interaction energy, ΔW, is given by the expression

$$\Delta W_m = W_m - W_{m\infty} = \pi\gamma \sum_{k=1}^{2} (h_k r_k \sin \psi_k - r_k^2)$$

$$- \Delta\rho g \int_{V_m} |z| \, dV - W_{m\infty}, \quad [3.7]$$

where $\Delta\rho = \rho_I - \rho_{II}$ and $W_{m\infty}$ is the limiting value of W_m for infinite interparticle separation. Here V_m is the volume comprised between the meniscus surface and its projection on the xy coordinate plane—see Fig. 1.

By means of some geometrical considerations one can represent Eq. [3.4] in the form

$$W_w = 2\pi \sum_{k=1}^{2} [\omega_{kI} R_k b_k + \omega_{kII} R_k (2R_k - b_k)]. \quad [3.8]$$

By using the Young equation

$$\omega_{kII} - \omega_{kI} = \gamma \cos \alpha_k, \quad k = 1, 2,$$

and Eq. [3.8], one can derive

$$\Delta W_w = -2\pi\gamma \sum_{k=1}^{2} R_k b_k \cos \alpha_k - W_{w\infty}, \quad [3.9]$$

where $W_{w\infty}$ is the limiting value of the first term in the right-hand side of Eq. [3.9] for $L \to \infty$ (cf. Fig. 1) and ΔW_w is the contribution of wetting into the capillary interaction energy.

Let $V_u^{(k)}$ be the volume of the upper part of the kth particle with respect to the level of the contact line of radius r_k (cf. Fig. 1). In view of Eqs. [3.2] and [3.3] one can represent the gravitational potential energy of phases I and II in the form

$$m_I g Z_I^{(c)} = \rho_I g \Big[\int_{V(z<0)} z dV + \int_{V_m} |z| \, dV + \sum_{k=1}^{2} (V_{cyl}^{(k)} |Z_{cyl}^{(k)}| - V_l^{(k)} Z_l^{(k)}) \Big] \quad [3.10]$$

$$m_{II} g Z_{II}^{(c)} = \rho_{II} g \Big[\int_{V(z>0)} z dV - \int_{V_m} |z| \, dV - \sum_{k=1}^{2} (V_{cyl}^{(k)} |Z_{cyl}^{(k)}| + V_u^{(k)} Z_u^{(k)}) \Big]. \quad [3.11]$$

Here $V_{cyl}^{(k)}$ is the volume of a cylinder of height h_k based on the contact line of the radius, r_k; $Z_{cyl}^{(k)}$, $Z_l^{(k)}$, and $Z_u^{(k)}$ are the z-coordinates of the mass centers of $V_{cyl}^{(k)}$, $V_l^{(k)}$, and $V_u^{(k)}$. Note that Eqs. [3.10] and [3.11] hold for the geometrical configurations depicted in both Figs. 1a and 1b. On the other

hand, the gravitational potential energy of the two floating particles can be expressed in the form

$$\sum_{k=1}^{2} m_k g Z_k^{(c)} = \sum_{k=1}^{2} \rho_k g (V_l^{(k)} Z_l^{(k)} + V_u^{(k)} Z_u^{(k)}), \quad [3.12]$$

supposing that particle k has a uniform density ρ_k.

On the other hand, $Z_{cyl}^{(k)} = h_k/2$. Then

$$V_{cyl}^{(k)} | Z_{cyl}^{(k)} | = \frac{\pi}{2} r_k^2 h_k^2. \quad [3.13]$$

In addition, since $Z_k^{(c)}$ is the z-coordinate of the sphere center, one can derive

$$V_l^{(k)} Z_l^{(k)} = V_l^{(k)} [Z_l^{(k)} - Z_k^{(c)}] + V_l^{(k)} Z_k^{(c)}$$

$$= -\frac{\pi}{4} r_k^4 + V_l^{(k)} Z_k^{(c)} \quad [3.14]$$

and

$$V_u^{(k)} Z_u^{(k)} = V_s^{(k)} Z_k^{(c)} - V_l^{(k)} Z_l^{(k)}$$

$$= V_s^{(k)} Z_k^{(c)} + \frac{\pi}{4} r_k^4 - V_l^{(k)} Z_k^{(c)}, \quad [3.15]$$

where

$$V_s^{(k)} = \frac{4}{3} \pi R_k^3 \quad [3.16]$$

is the volume of the respective sphere. By substituting from Eqs. [3.10]–[3.15] into Eq. [3.2] one obtains

$$W_g = \Delta\rho g \left\{ \int_{V_m} |z| \, dV + \sum_{k=1}^{2} \left[(D_k V_s^{(k)} - V_l^{(k)}) Z_k^{(c)} + V_{cyl}^{(k)} | Z_{cyl}^{(k)} | + \frac{\pi}{4} r_k^4 \right] \right\} \quad [3.17]$$

within the accuracy of an additive constant, which does not depend on the interparticle distance L; here

$$D_k = (\rho_k - \rho_{II})/\Delta\rho, \quad \Delta\rho = \rho_I - \rho_{II}. \quad [3.18]$$

From Eqs. [3.13] and [3.17] one derives an expression for the gravity contribution to the interaction energy:

$$\Delta W_g = \Delta\rho g \left\{ \int_{V_m} |z| \, dV + \sum_{k=1}^{2} \left[(D_k V_s^{(k)} - V_l^{(k)}) Z_k^{(c)} + \frac{\pi}{4} r_k^2 (r_k^2 + 2h_k^2) \right] \right\} - W_{g\infty}, \quad [3.19]$$

where $W_{g\infty}$ is the limiting value of W_g, as given by Eq. [3.17], for $L \to \infty$.

Finally, the combination of Eqs. [3.6], [3.7], [3.9], and [3.19] yields an expression for the capillary interaction energy:

$$\Delta W = \Delta\rho g \sum_{k=1}^{2} \left[(D_k V_s^{(k)} - V_l^{(k)}) Z_k^{(c)} + \frac{\pi}{4} r_k^2 (r_k^2 + 2h_k^2) \right] + \pi\gamma \sum_{k=1}^{2} (h_k r_k \sin\psi_k - r_k^2 - 2R_k b_k \cos\alpha_k) - W_\infty, \quad [3.20]$$

where $W_\infty = W_{m\infty} + W_{w\infty} + W_{g\infty}$ is constant with respect to the interparticle separation L and $Z_k^{(c)}$, $V_l^{(k)}$, and r_k can be calculated from Eqs. [2.2]–[2.4].

4. THE VERTICAL FORCE BALANCE

Let us consider the forces exerted on a spherical particle, floating attached to an interface at equilibrium. The vertical force due to the meniscus surface tension γ is counterbalanced by the gravity force (see, e.g., Eqs. [26] and [32] in Ref. 12):

$$2\pi\gamma r_k \sin\psi_k = F_g^{(k)}, \quad k = 1, 2, \quad [4.1]$$

where the gravity force

$$F_g^{(k)} = g[(\rho_I - \rho_k) V_l^{(k)} + (\rho_{II} - \rho_k) V_u^{(k)} - \Delta\rho \pi r_k^2 h_k] \quad [4.2]$$

is in fact the difference between the upthrust and the particle weight.

Since $V_l^{(k)} + V_u^{(k)} = V_s^{(k)}$, by using Eq. [3.18] one can transform Eq. [4.2] to read

$$F_g^{(k)} = \gamma q^2 (V_l^{(k)} - D_k V_s^{(k)} - \pi r_k^2 h_k), \quad [4.3]$$

where

$$q^2 = \Delta\rho g/\gamma. \quad [4.4]$$

Equation [4.1] shows that the sign of ψ_k is determined by the sign of $F_g^{(k)}$: when the upthrust predominates ψ_k is positive; when the particle weight predominates ψ_k is negative. When the particle is too heavy, the balance, Eq. [4.1], can be violated and the particle will detach from the interface. Indeed, the left-hand side of Eq. [4.1] is limited. One can prove that the quantity

$$Q_k = r_k \sin\psi_k \quad [4.5]$$

has bounded variation: from the condition for extremum,

$$0 = \frac{dQ_k}{d\psi_k} = \frac{d}{d\psi_k}[R_k \sin(\alpha_k + \psi_k)\sin\psi_k],$$

(R_k = const, α_k = const), one can derive (see, e.g., Ref. 13)

$$-R_k \sin^2\frac{\alpha_k}{2} \leqslant Q_k \leqslant R_k \cos^2\frac{\alpha_k}{2}. \qquad [4.6]$$

By using Eqs. [2.2], [2.3], [3.16], [4.1], [4.3], and [4.4], one can represent Eq. [3.20] in the form

$$\Delta W = \Delta W_w + \Delta\tilde{W}_m + \Delta\tilde{W}_g, \qquad [4.7]$$

where

$$\Delta\tilde{W}_m = \pi\gamma \sum_{k=1}^{2}(h_k r_k \sin\psi_k - r_k^2) - \tilde{W}_{m\infty} \qquad [4.8]$$

$$\Delta\tilde{W}_g = -\pi\gamma \sum_{k=1}^{2}\{2h_k r_k \sin\psi_k - q^2[\tfrac{1}{4}r_k^2(r_k^2 - 2h_k^2) + (\tfrac{4}{3}D_k R_k^3 - R_k b_k^2 + \tfrac{1}{3}b_k^3)(R_k - b_k)]\} - \tilde{W}_{g\infty} \qquad [4.9]$$

—cf. Eqs. [3.7] and [3.19] (the integrals over the meniscus volume, V_m, are omitted in Eqs. [4.8], [4.9] due to their cancellation in the total interaction energy—Eqs. [3.20] and [4.7]). The constants $\tilde{W}_{m\infty}$ and $\tilde{W}_{g\infty}$ are chosen in such a way that for $L \to \infty$ both $\Delta\tilde{W}_m$ and $\Delta\tilde{W}_g$ tend to zero. Equations [3.9], [4.8], and [4.9] will be used below to calculate the contributions of wetting, meniscus surface tension, and gravity into the energy of capillary interaction between the two particles. However, before that we need some expressions for the contact line elevation h_k.

5. ELEVATION OF THE CONTACT LINES

It is not possible to calculate numerical values of the capillary interaction energy ΔW without solving the Laplace equation for the meniscus profile and finding the elevations h_1 and h_2. In this paper we restrict our considerations to small particles; i.e.,

$$(qR_k)^2 \ll 1, \quad k = 1, 2. \qquad [5.1]$$

For example, in the case of a water–air interface, $q^{-1} = 2.7$ mm and Eq. [5.1] implies $R_k \leqslant 850$ μm. It was proven by Chan *et al.* (7) that when Eq. [5.1] is satisfied, the meniscus slope is small; i.e.,

$$\left(\frac{\partial\zeta}{\partial x}\right)^2 \ll 1, \left(\frac{\partial\zeta}{\partial y}\right)^2 \ll 1. \qquad [5.2]$$

In this case the Laplace equation can be linearized and analytical expressions for h_k can be obtained. Here we make use of the asymptotic expressions derived in Ref. (10) for $(qL)^2 \ll 1$:

$$h_k = Q_k\{\tau_k + 2\ln[1 - \exp(-2\tau_k)]\} - (Q_1 + Q_2)\ln(\gamma_e qa) + (Q_1 - Q_2) \times\left[A - (-1)^k \sum_{n=1}^{\infty}\frac{2}{n}\frac{\exp(-n\tau_k)\sinh n\tau_j}{\sinh n(\tau_1 + \tau_2)}\right], \quad j, k = 1, 2, j \neq k, \qquad [5.3]$$

where Q_1 and Q_2 are given by Eq. [4.5] above, $\gamma_e = 1.781072418\cdots$ ($\ln\gamma_e$ is the constant of Euler–Masceroni—see e.g. Ref. 15), and

$$A = \sum_{n=1}^{\infty}\frac{1}{n}\frac{\sinh n(\tau_1 - \tau_2)}{\sinh n(\tau_1 + \tau_2)} \qquad [5.4]$$

$$\tau_k = \ln(a/r_k + \sqrt{a^2/r_k^2 + 1}), \quad k = 1, 2, \qquad [5.5]$$

$$a^2 = [L^2 - (r_1 + r_2)^2][L^2 - (r_1 - r_2)^2]/(2L)^2. \qquad [5.6]$$

For two identical particles ($R_1 = R_2$, $\alpha_1 = \alpha_2$), Eq. [5.3] reduces to

$$h_k = Q_k\tau_k + 2Q_k\ln\frac{1 - \exp(-2\tau_k)}{\gamma_e qa}, \quad k = 1, 2. \qquad [5.7]$$

The elevation of the contact line at infinite interparticle separation (single particle) can be determined by means of Derjaguin's (14) formula:

$$h_{k\infty} = r_{k\infty}\sin\psi_{k\infty}\ln\frac{4}{\gamma_e q r_{k\infty}(1 + \cos\psi_{k\infty})}, \quad k = 1, 2; (qr_{k\infty})^2 \ll 1. \qquad [5.8]$$

Here and subsequently the subscript "∞" denotes the value of the respective parameter for $L \to \infty$. In our case Eq. [5.2] holds; i.e., the meniscus slope is small and one can set $\cos\psi_{k\infty} \approx 1$ in Eq. [5.8].

For $r_k \ll L$ and using Eqs. [5.3] and [5.8] one can write (Ref. (10), Eq. [B.11])

$$h_k = h_{k\infty} + Q_j K_0(qL); \quad j, k = 1, 2, j \neq k; r_k \ll L, \qquad [5.9]$$

where K_0 is the modified Bessel function of zero-th order. In view of the asymptotic formula (15, 16)

$$K_0(x) = \ln\frac{2}{\gamma_e x} + O(x^2\ln x), \quad x \to 0, \qquad [5.10]$$

Eq. [5.9] yields

$$h_k = h_{k\infty} + Q_j \ln \frac{2}{\gamma_e q L};$$

$$j, k = 1, 2, j \neq k, r_k \ll L \ll q^{-1}. \quad [5.11]$$

One can also calculate the shape of the liquid meniscus around the two floating particles by using Eqs. [2.35]–[2.39] in Ref. (10), or Eqs. [3.49]–[3.52] in Ref. (9).

6. ASYMPTOTIC EXPRESSIONS FOR THE CAPILLARY FORCES

Having in mind Eqs. [5.1] and [5.2], one can derive from Eqs. [4.1], [4.2], and [5.8]

$$|Q_k|/R_k \sim (qR_k)^2 \ll 1, \quad [6.1]$$

$$|h_k/R_k| \sim (qR_k)^2 |\ln qR_k| \ll 1, \quad k = 1, 2. \quad [6.2]$$

Then after some mathematics (see the Appendix) one can prove that

$$\frac{db_k}{dL} = -r_k \frac{d\psi_k}{dL} = -\frac{dQ_k}{dL}[1 + O(q^2R_k^2)]$$

$$= \frac{1}{2}(qr_k)^2 \frac{dh_k}{dL}[1 + O(q^2R_k^2)]. \quad [6.3]$$

From Eqs. [2.4], [3.9], [4.8], and [4.9] one derives

$$\frac{d\Delta W_w}{dL} = -\pi\gamma \sum_{k=1}^{2} (qr_k)^2 R_k \cos\alpha_k \frac{dh_k}{dL} \times [1 + O(q^2R_k^2)] \quad [6.4]$$

$$\frac{d\Delta \tilde{W}_m}{dL} = \pi\gamma \sum_{k=1}^{2} [Q_k + (qr_k)^2 R_k \cos\alpha_k] \frac{dh_k}{dL} \times [1 + O(q^2R_k^2)] \quad [6.5]$$

$$\frac{d\Delta \tilde{W}_g}{dL} = -\pi\gamma \sum_{k=1}^{2} 2Q_k \frac{dh_k}{dL}[1 + O(q^2R_k^2)]. \quad [6.6]$$

Combining Eqs. [6.4]–[6.6] in accordance with Eq. [4.7] yields an asymptotic expression for the lateral capillary force

$$F = \frac{d(\Delta W)}{dL} = -\pi\gamma \sum_{k=1}^{2} Q_k \frac{dh_k}{dL}[1 + O(q^2R_k^2)]. \quad [6.7]$$

It is interesting to note that the contribution of the wetting energy, $d(\Delta W_w)/dL$, in spite of being comparable with the gravity and meniscus surface contributions, is canceled by a part of $d(\Delta \tilde{W}_m)/dL$—cf. Eqs. [6.4] and [6.5]. Besides, the rest of the meniscus contribution, $d(\Delta \tilde{W}_m)/dL$, is canceled by the half of the gravity contribution, $d(\Delta \tilde{W}_g)/dL$—see Eqs. [6.5], [6.6]. Thus the capillary force, F, turns out to be approximately equal to the half of the gravity contribution $d(\Delta \tilde{W}_g)/dL$, just as intuitively assumed by Nicolson (6) long ago.

Substituting Eq. [5.9] into Eq. [6.7], one obtains

$$F = 2\pi\gamma Q_1 Q_2 q K_1(qL)[1 + O(q^2R_k^2)], \quad r_k \ll L, \quad [6.8]$$

where K_1 is the modified Bessel function of the first order. In addition, from [6.7]–[6.8] one derives an asymptotic expression for the energy of capillary interaction:

$$\Delta W = -2\pi\gamma Q_1 Q_2 K_0(qL)[1 + O(q^2R_k^2)], \quad r_k \ll L. \quad [6.9]$$

In view of the above discussion it is not surprising that the asymptotic expressions, Eqs. [6.8] and [6.9], are equivalent to Eqs. [33] and [34] of Ref. (7), derived by using the approach due to Nicolson.

For $L > q^{-1}$ the functions $K_0(qL)$ and $K_1(qL)$ decay exponentially—see e.g. Ref. (16). That is why one can say that the capillary length q^{-1} determines the range of the lateral capillary interactions. For $(qL)^2 \ll 1$ (that is $L \ll 850$ μm for the water–gas interface), when the capillary interactions become important, Eqs. [6.8] and [6.9] reduce to

$$F = 2\pi\gamma \frac{Q_1 Q_2}{L}, \quad r_k \ll L \ll q^{-1} \quad [6.10]$$

$$\Delta W = 2\pi\gamma Q_1 Q_2 \ln(\gamma_e qL/2), \quad r_k \ll L \ll q^{-1}. \quad [6.11]$$

Here we have used Eq. [5.10] and the analogous expression for $K_1(x)$ (15, 16):

$$K_1(x) = \frac{1}{x} + O(x \ln x), \quad x \to 0. \quad [6.12]$$

The form of Eq. [6.10] resembles Newton's law of gravity or Coulomb's law of electricity, irrespective of the different power of the distance, L. The counterparts of the particle masses or charges, Q_1 and Q_2, are in fact proportional to the gravity force—cf. Eqs. [4.1] and [4.5]. In view of Eq. [6.3] for small particles Q_1 and Q_2 depend weakly on L. Therefore one can use in Eqs. [6.7]–[6.11] the limiting values of Q_1 and Q_2 calculated by Chan *et al.* (7):

$$Q_k \approx Q_{k\infty} = \tfrac{1}{6} q^2 R_k^3 (2 - 4D_k + 3\cos\alpha_k - \cos^3\alpha_k) \times [1 + O(qR_k)] \quad [6.13]$$

(Eq. [6.13] is a corollary of Eq. [27] in Ref. 7). When using Eq. [6.13] to calculate Q_k one should keep in mind that only

those values of Q_k which satisfy Eq. [4.6] correspond to equilibrium attachment of the particle to the interface. Hence, the effective "capillary charge" Q_k is a quantity of bounded variation, which can be both positive and negative. Correspondingly, the capillary force F in Eq. [6.10] is attractive when $Q_1Q_2 > 0$ and repulsive when $Q_1Q_2 < 0$. In addition, Eq. [6.13] shows that in zero-th order approximation Q_k is determined by the capillary length q^{-1}, density ratio D_k, and particle radius and contact angle, R_k and α_k. The strong dependence of Q_k on R_k leads to a fast decay of the capillary force with the decrease of the particle radii: for two identical particles Eqs. [6.8] and [6.9] yield

$$F \propto R^6 K_1(qL) \quad (R_1 = R_2 = R,\ r_k \ll L) \qquad [6.14]$$

$$\Delta W \propto -R^6 K_0(qL) \quad (R_1 = R_2 = R,\ r_k \ll L). \qquad [6.15]$$

Equations [6.11] and [6.13] allow us to estimate the critical particle size at which the capillary interaction energy becomes comparable with the energy of the thermal fluctuations, $\Delta W/kT \sim 1$. Since $\cos \alpha_k \sim 1$ and $D_k \sim 1$, one can write

$$\Delta W \sim \gamma q^4 R_1^3 R_2^3 \ln(qL), \quad qL \ll 1. \qquad [6.16]$$

For similar particles ($R_1 = R_2 = R$), $\Delta W/kT \sim 1$ for particle size

$$qR \sim \sqrt[6]{\frac{kTq^2}{\gamma \ln(qL)}}, \quad \Delta W/kT \sim 1. \qquad [6.17]$$

For typical values of the parameters $q \sim 10\ \text{cm}^{-1}$, $\gamma \sim 50$ mN/m, and $L \sim R$, one obtains

$$qR \sim 10^{-2}, \quad \Delta W/kT \sim 1. \qquad [6.18]$$

This means that the capillary interaction between particles floating attached to an interface becomes negligible for particle size smaller than ca. 10 μm. This estimate is confirmed by the numerical results presented in Section 8. However, as discussed in Ref. (9), this is not the case for particles protruding from a liquid layer on a solid substrate, when the capillary interactions can be significant even for $R \sim 10$ nm (see Fig. 12 and the discussion in Section 8 below).

Before presenting the numerical results in more detail, we describe briefly the procedure of calculations.

7. PROCEDURE OF CALCULATIONS

Our aim is to calculate the energy of capillary interaction, ΔW, and the capillary force, $F = d(\Delta W)/dL$, from the general expressions Eqs. [4.7]–[4.9]. We suppose that the material parameters γ, q, D_k, and α_k and the geometrical parameters R_k and L are known ($k = 1, 2$).

Using some geometrical considerations, one obtains the expression (cf. Fig. 1):

$$\psi_k = \arccos\left(\frac{b_k}{R_k} - 1\right) - \alpha_k, \quad k = 1, 2. \qquad [7.1]$$

Besides, from Eqs. [2.3], [3.16], [4.1], [4.3], and [4.5] one derives

$$Q_k = \tfrac{1}{2}q^2[b_k^2(R_k - b_k/3) - \tfrac{4}{3}D_k R_k^3 - r_k^2 h_k]. \qquad [7.2]$$

Then Eqs. [2.4], [4.5], [5.3], [7.1], and [7.2] for $k = 1, 2$ form a set of 10 equations for the 10 unknown variables r_k, Q_k, h_k, ψ_k, and b_k ($k = 1, 2$). When the two particles are identical the above problem reduces to a set of five equations for five variables; in this case Eq. [5.7] can be used instead of Eq. [5.3]. If $qL \geqslant 1$, Eq. [5.9] must be used instead of Eq. [5.3] or [5.7]. To determine W_∞ one needs also the limiting values $r_{k\infty}$, $Q_{k\infty}$, $h_{k\infty}$, $\psi_{k\infty}$, and $b_{k\infty}$ for $L \to \infty$. The latter can be determined by means of the same set of five equations in which Eq. [5.7] is exchanged with Eq. [5.8].

In all cases the problem was solved numerically. Then ΔW was calculated from Eqs. [3.9] and [4.7]–[4.9] and $F = d(\Delta W)/dL$ was determined by numerical differentiation.

For $R_k \leqslant 850$ μm one can use a much faster iterative procedure, which is described below. Since in the present paper we deal with the case of small meniscus slope, i.e., Eq. [5.2] holds, one can write

$$r_k = R_k \sin(\alpha_k + \psi_k) \approx R_k \cos \alpha_k \sin \psi_k + R_k \sin \alpha_k. \qquad [7.3]$$

The substitution of $\sin \psi_k$ from Eq. [4.5] into Eq. [7.3] leads to a quadratic equation for r_k, whose solution reads

$$r_k = \tfrac{1}{2}[R_k \sin \alpha_k + (R_k^2 \sin^2 \alpha_k + 4Q_k R_k \cos \alpha_k)^{1/2}]. \qquad [7.4]$$

In addition, from Eq. [6.3] one obtains

$$Q_k^{(n+1)} = Q_k^{(n)} - \tfrac{1}{2}(qr_k)^2(h_k^{(n+1)} - h_k^{(n)}), \quad k = 1, 2, \qquad [7.5]$$

where $Q_k^{(n+1)}$ and $Q_k^{(n)}$ are two consecutive approximations for Q_k (the same for $h_k^{(n+1)}$ and $h_k^{(n)}$); $n = 0, 1, 2, \ldots$.

(i) To start the iterations one can use $r_k^{(0)} = r_{k\infty}$, $Q_k^{(0)} = Q_{k\infty}$, and $h_k^{(0)} = h_{k\infty}$, where $Q_{k\infty}$ is determined from Eq. [6.13], $r_{k\infty}$ is then calculated from Eq. [7.4] with $Q_k = Q_{k\infty}$, and finally $h_{k\infty}$ is determined from Eq. [5.8].

(ii) $h_k^{(n+1)}$ is calculated from Eq. [5.3] by substituting $Q_k = Q_k^{(n)}$ and $r_k = r_k^{(n)}$.

(iii) Then Eq. [7.5] provides the next approximation, $Q_k^{(n+1)}$, which substituted in Eq. [7.3] yields $r_k^{(n+1)}$. After that step, step (ii) is repeated again to give $h_k^{(n+2)}$, etc.

This simple iterative procedure is quickly convergent. With the values of Q_k, r_k, and h_k ($k = 1, 2$) thus obtained one then calculates

$$\psi_k = \arcsin(Q_k/r_k), \quad b_k = R_k[1 + \cos(\alpha_k + \psi_k)]. \quad [7.6]$$

Finally, from Eqs. [3.9] and [4.7]–[4.9] one determines ΔW.

For $R_k \leqslant 100\ \mu$m one can use also Eq. [6.7] and its counterpart

$$\Delta W = -\pi\gamma \sum_{k=1}^{2} (Q_k h_k - Q_{k\infty} h_{k\infty})[1 + O(q^2 R_k^2)] \quad [7.7]$$

to determine the capillary interaction force and energy. Note that Eqs. [6.7] and [7.7], coupled with Eq. [5.3], are more general than Eqs. [6.8]–[6.9], the latter being subject to the additional restriction $L \gg r_k$.

8. NUMERICAL RESULTS AND DISCUSSION

First of all let us compare the capillary force $F = d(\Delta W)/dL$, calculated by numerical differentiation of Eq. [4.7] (along with Eqs. [3.9], [4.8], and [4.9]), with the capillary force as given by Eqs. [6.8] and [6.13], which are due to Chan *et al.* (7). For that purpose, let us consider the ratio of these two forces

$$\Phi = \frac{F(\text{Eq. [4.7]})}{F(\text{Eq. [6.8]})}. \quad [8.1]$$

The plot of Φ vs $L/(2R)$ is shown in Fig. 2 for a specified choice of the parameters: $R_1 = R_2 = 10\ \mu$m, $\rho_1 = \rho_2 = 3$ g/cm^3, $\rho_I = 1$ g/cm^3, $\rho_{II} = 0$, $\gamma = 70$ mN/m, and the contact angle $\alpha_1 = \alpha_2 = \alpha$ is varied. For large distance L between

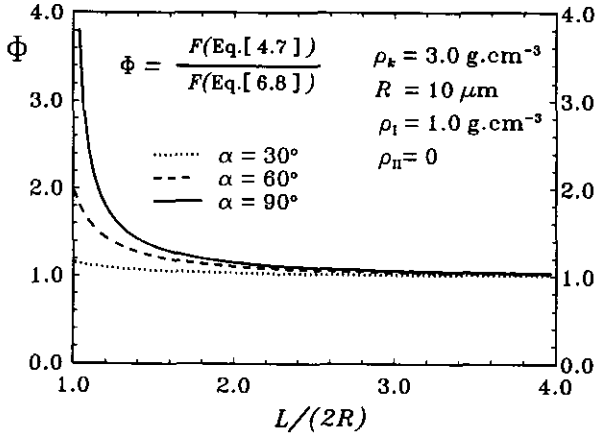

FIG. 2. Plot of the ratio Φ of the capillary force, calculated by differentiation of Eq. [4.7] and the force calculated by means of the asymptotic formula, Eq. [6.8]. The dotted, dashed, and solid lines correspond to three-phase contact angles 30°, 60°, ad 90°, respectively.

TABLE 1

Comparison between the Capillary Force $F_x^{(k)}$ and the Derivative $d(\Delta W)/dL$ for Two Floating Microparticles Attached to an Air/Water Interface with $\gamma = 70$ mN/m

L (μm)	ΔW (J)	$F_x^{(k)}$ (N)	$d(\Delta W)/dL$
20.0	-3.30×10^{-20}	3.83×10^{-16}	3.21×10^{-16}
40.0	-2.81×10^{-20}	1.69×10^{-16}	1.61×10^{-16}
60.0	-2.54×10^{-20}	1.10×10^{-16}	1.07×10^{-16}
80.0	-2.35×10^{-20}	8.18×10^{-17}	8.09×10^{-17}
100.0	-2.21×10^{-20}	6.52×10^{-17}	6.47×10^{-17}

Note. $R_1 = 15\ \mu$m, $\alpha_1 = 10°$, $\rho_1 = 3.0$ g/cm^3; $R_2 = 5\ \mu$m, $\alpha_2 = 20°$, $\rho_2 = 3.0$ g/cm^3.

the two particles, Φ tends to 1. This could be expected because Eq. [6.8] is derived by using the assumption $L \gg R_k$. On the other hand, for shorter interparticle distances, say $L/(2R) \leqslant 3$, Φ is pronouncedly larger than 1, which means that Eq. [6.8] considerably underestimates the magnitude of the capillary forces in this case. Since $(qR)^2 \ll 1$, our Eq. [6.7], coupled with Eq. [5.3], turns out to give the same numerical results as the differentiated Eq. [4.7]. Besides, the deviation of Φ from 1 increases when the contact angle α is approaching 90°.

In Ref. (10) an independent force approach for calculating the capillary forces was developed (see the comments on Eq. [8.3] below). It is proven there that the magnitudes of the horizontal projections of the capillary forces, exerted on the two particles, must be equal: $F_x^{(1)} = F_x^{(2)}$. In Table 1 we compare the values of $F_x^{(k)}$ determined by means of the force approach (Eqs. [6.1], [6.14], [6.20], [6.22], and [6.23] of Ref. 10) with $F = d(\Delta W)/dL$ due to the energetical approach; i.e., calculated by means of Eq. [4.7] above. As seen in Table 1 the numerical results of the two approaches are in a good agreement in spite of the approximations, like Eqs. [5.1] and [5.2], used in both approaches. It should be also noted that although $\alpha_1 \neq \alpha_2$ and $R_1 \neq R_2$ the force approach of Ref. (10) yields $F_x^{(1)} = F_x^{(2)}$, as it must be.

Table 1 contains also data for the capillary interaction energy ΔW vs L calculated by means of Eq. [4.7]. One can see that ΔW is negative (attraction between the two spheres) and the magnitude of ΔW is of the order of 3–5 times the thermal energy kT. Besides, $|\Delta W|$ decays with the increase of the interparticle distance. This is illustrated graphically for two identical particles in Fig. 3, where L is plotted in a logarithmic scale. The straight lines means that for a wide range of distances the asymptotic formula, Eq. [6.11], holds. (However, for $L \gg q^{-1}$, ΔW decays much faster (exponentially) in accordance with Eq. [6.9]; in addition, for $L \sim r_k$, when $\Phi \neq 1$ (cf. Fig. 2), Eq. [6.11] also does not hold.)

Figure 3 illustrates also the strong dependence of the energy of capillary interaction on the density of the two particles. One sees that when $R_1 = R_2 = 10\ \mu$m there is no capillary

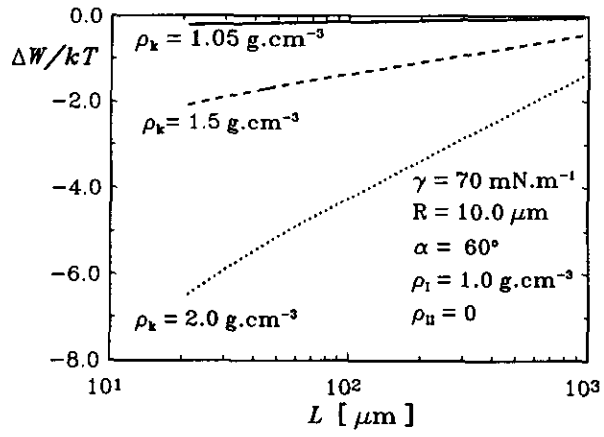

FIG. 3. Dependence of the capillary interaction energy, $\Delta W/kT$, on the interparticle distance, L, for three different values of the particle mass density, ρ_k.

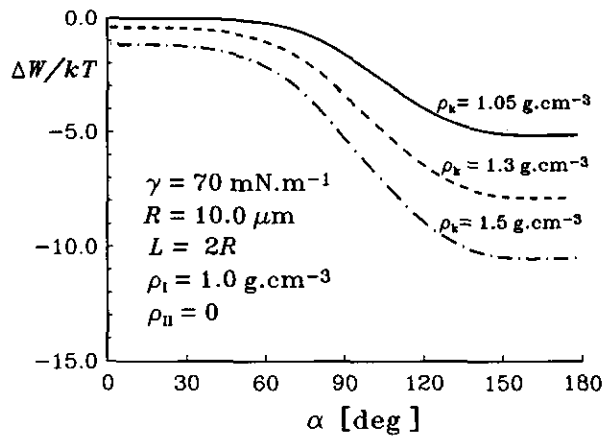

FIG. 5. Plot of $\Delta W/kT$ vs α for different values of ρ_k. The other parameters are the same as in Fig. 4.

interaction between two particles of density $\rho_k = 1.05$ g/cm^3 ($|\Delta W| \leq kT$), however there is a pronounced interaction when $\rho_k = 2$ g/cm^3.

Figure 4 provides a closer examination of the density dependence of ΔW for different values of the contact angle $\alpha = \alpha_1 = \alpha_2$ of two identical particles. To specify the value of L we have chosen $L = 2R$; i.e., the particles (but not the three-phase contact lines) are in close contact. As could be expected, ΔW is negative (attraction); however, for some value of ρ_k, ΔW is zero and the respective curve in Fig. 4 exhibits a maximum. The latter corresponds to $Q_k = 0$; i.e., to nondeformed (flat) liquid surface. The density $\rho_k = \rho_k^*$ in this special case can be estimated from Eqs. [3.18] and [6.13]:

$$\frac{\rho_k^* - \rho_{II}}{\rho_I - \rho_{II}} = \tfrac{1}{4}(2 + 3\cos\alpha_k - \cos^3\alpha_k). \qquad [8.2]$$

Figure 5 illustrates the dependence of the capillary interaction energy, ΔW, on the contact angle, α_k, for two identical particles of the same size, like those in Fig. 4. The effect of α_k turns out to be pronounced in the interval $45° < \alpha_k < 135°$; outside this interval ΔW is almost constant. This behavior is due to the fact that the "capillary charge," Q_k, depends on α_k via $\cos\alpha_k$, cf. Eq. [6.13], and $\cos\alpha_k$ varies strongly in the interval $45° < \alpha_k < 135°$, whereas $\cos\alpha_k$ is alsmost constant (± 1) outside this interval.

Figure 6 illustrates the effect of surface tension γ on the capillary interaction between two floating particles. One can see that the lower the γ, the greater the magnitude $|\Delta W|$ of the capillary interaction energy. From Eqs. [4.4] and [6.13] one finds that the "capillary charge" of a floating particle is inversely proportional to the surface tension: $Q_k \propto 1/\gamma$. Then from Eq. [6.9] one obtains $\Delta W \propto \gamma Q_1 Q_2 \propto 1/\gamma$—this explains the behavior of the curves in Fig. 6. In other words, the lower the surface tension γ, the greater the surface deformation (characterized by Q_k) and the greater

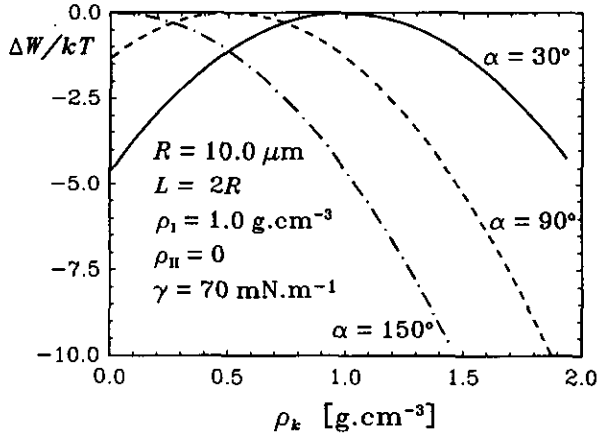

FIG. 4. Plot of $\Delta W/kT$ vs particle mass density, ρ_k, for two similar particles with radii of 10 μm, in contact, for different values of the contact angle, α.

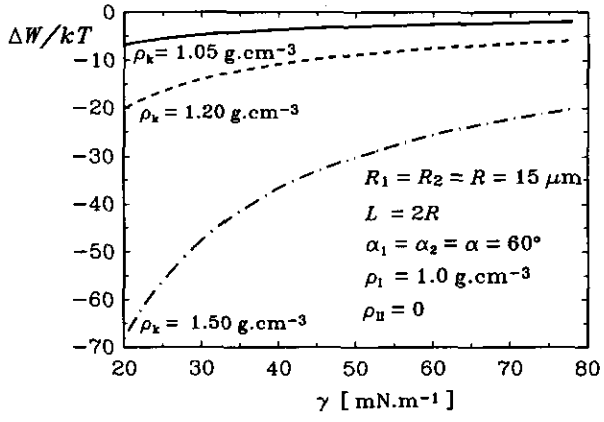

FIG. 6. Dependence of $\Delta W/kT$ on the interfacial tension, γ, for similar particles with radii of 15 μm and a three-phase contact angle of 60°. The curves correspond to different values of the particle mass density, ρ_k.

the capillary interaction. Such behavior was first reported by Chan *et al.* (7).

In contrast with Figs. 3–6, Fig. 7 presents data for the capillary interaction between two different particles ($R_1 \neq R_2$, $\alpha_1 \neq \alpha_2$). $R_2 = 5$ μm is kept constant and R_1 is varied. One can see that, for $R_1 = 5$ μm, $|\Delta W| < kT$ and the capillary interaction between the particles is negligible. However, for $R_1 = 15$ μm, $|\Delta W| \sim 10kT$ and a pronounced interparticle attraction takes place.

When $Q_1Q_2 < 0$, the particles repel each other ($\Delta W > 0$). Such is the case of a floating bubble and a floating heavier particle, illustrated in Fig. 8. The bubble radius is fixed, $R_2 = 20$ μm, and the solid particle radius is varied. As could be expected, the larger the particle radius, the greater the capillary repulsion.

Figure 9 illustrates the magnitude and the sign of the different components of the capillary interaction energy, ΔW. The wetting component ΔW_w is calculated from Eq. [3.9]. The meniscus and gravity components, $\Delta \tilde{W}_m$ and $\Delta \tilde{W}_g$, are calculated from Eqs. [4.8] and [4.9]. The total capillary interaction energy, ΔW, is a superposition of all these components, in accordance with Eq. [4.7]. One sees in Fig. 9 that the contributions of all components have comparable magnitudes but different signs. One can see also that the total energy, ΔW, turns out to be approximately equal to half of the gravitational energy, $\Delta \tilde{W}_g$, as discussed after Eq. [6.7] above.

Just like in the *energetical* approach, ΔW has gravitational, meniscus, and wetting components; in the *force* approach, developed in Ref. (10), the lateral capillary force $F_x^{(k)}$ exerted on the kth particle ($k = 1, 2$) has pressure and surface tension components:

$$F_x^{(k)} = F_x^{(kp)} + F_x^{(k\gamma)}, \quad k = 1, 2. \qquad [8.3]$$

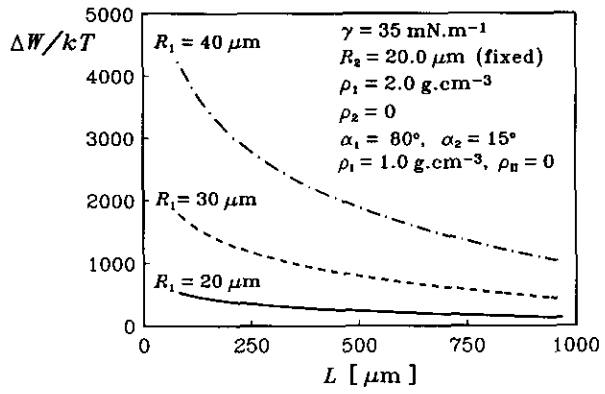

FIG. 8. Dependence of $\Delta W/kT$ on L in the case of heavy particle–bubble capillary repulsion. The equatorial radius of the bubble $R_2 = 20$ μm is fixed and the particle radius, R_1, is varied.

$F_x^{(kp)}$ is related to the integral of the hydrostatic pressure over the surface of the particle and $F_x^{(k\gamma)}$ is related to the integral of the surface tension γ along the contact line—see Eqs. [6.2] and [6.3] in Ref. (10). Our aim now is to compare the magnitudes of $F_x^{(k\gamma)}$ and $F_x^{(kp)}$ in the case of two floating spherical particles. The parameters r_k, ψ_k, and h_k can be determined as explained in the previous section. Then one can calculate $F_x^{(kp)}$ and $F_x^{(k\gamma)}$ from Eqs. [6.14] and [6.20] in Ref. (10). The ratio $F_x^{(kp)}/F_x^{(k\gamma)}$ is plotted in Fig. 10 vs the distance L between two identical spherical particles of radius R. One sees that $F_x^{(kp)} \ll F_x^{(k\gamma)}$, so the contribution of the pressure to the lateral capillary force turns out to be negligible for submillimeter particles. Similar is the situation of the case of two spheres protruding from a liquid layer on a solid substrate investigated in Ref. (10).

Finally let us consider the dependence of the capillary interactions on the particle radius. As an illustration, Fig. 11 presents the plot of the energy ΔW vs particle radius. The two particles are supposed to be identical: $R_1 = R_2 = R$, α_1

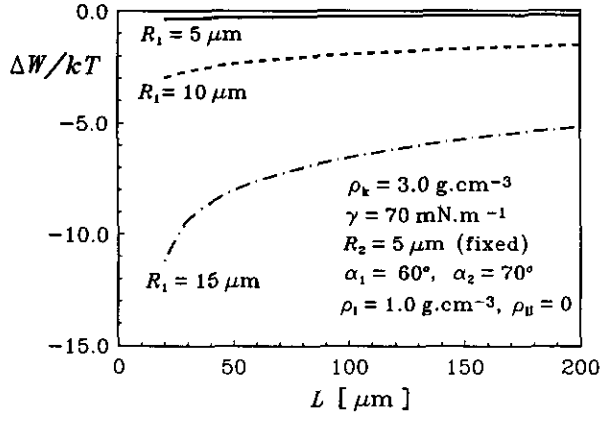

FIG. 7. Dependence of $\Delta W/kT$ on L for particles that differ in size and contact angle. The contact angles are $\alpha_1 = 60°$, $\alpha_2 = 70°$. The radius $R_2 = 5$ μm is kept constant, whereas R_1 is varied. The two particles are of equal mass density, $\rho_k = 3.0$ g/cm^3.

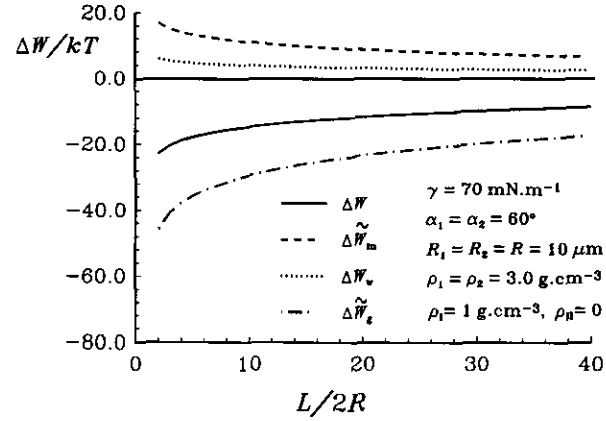

FIG. 9. Plot of the different contributions (gravitational, wetting, and meniscus) to the interaction energy, ΔW (see Eqs. [3.9] and [4.7]–[4.9]).

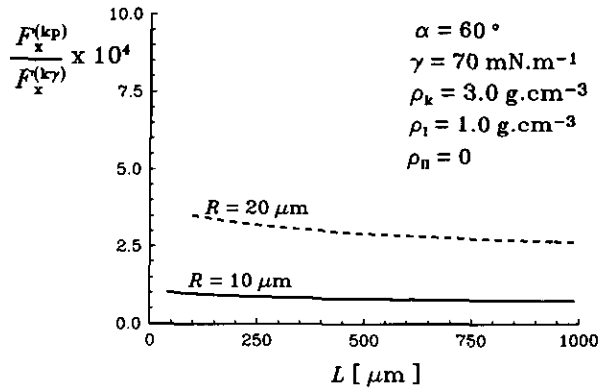

FIG. 10. Plot of $F_x^{(kp)}/F_x^{(k\gamma)}$ vs L for two identical particles of mass density $\rho_k = 3.0$ g/cm^3 and contact angle $\alpha = 60°$. The solid and dashed curves correspond to radii $R = 10$ μm and $R = 20$ μm, respectively.

$= \alpha_2 = \alpha = 60°$. It is seen that ΔW decays quickly with the decrease of R. For $R < 10$ μm the lateral capillary interaction between two floating particles becomes negligible. Such behavior could be expected in view of Eqs. [6.17] and [6.18] above.

In general, the capillary attraction between two similar floating particles appears because the liquid meniscus deforms in such a way that the gravitational potential energy of the two particles decreases when they approach each other. Thus it is not surprising that in the case of small particles ($qR_k < 10^{-2}$), when the particle gravitational energy is small, both the meniscus deformation and the capillary interaction are negligible.

However, the situation is quite different when the particles (instead of being floating) are restricted in their vertical movement by the presence of a solid substrate (9, 10). We call such a configuration "particles partially immersed in a liquid layer on a substrate" and the respective forces "immersion capillary forces". As shown in Refs. (9, 10) in the latter case the energy of capillary attraction turns out to be much larger than kT even with submicrometer particles. This effect is related to the three-phase contact angle; i.e., to the intermolecular forces, rather than to gravity.

Figure 12 illustrates the difference between these two cases: (i) of floating particles (the dashed line) and (ii) of particles partially immersed in a liquid layer on a solid substrate (the solid line). The plot represents the dependence of $\Delta W/kT$ on the particle radius, R, for two identical particles, $R_1 = R_2 = R$, $\alpha_1 = \alpha_2 = \alpha = 60°$, $\rho_1 = \rho_2 = \rho_p$. It is supposed that in case (ii) the thickness of the liquid layer, l_0, is equal to the particle radius, R. In both cases the particles are considered to be in contact; i.e., $L = 2R$. It is seen that the presence of a solid substrate increases the magnitude of capillary interaction by several orders of magnitude. There is experimental evidence (17–19) that such "immersion" capillary forces can bring about the formation of a two-dimensional array (2D-colloid crystal) from both micrometer-sized and submicrometer particles: e.g., latex spherical particles, protein globules, etc.

9. CONCLUDING REMARKS

The main results in this paper can be summarized as follows:

(i) A general approach based on an expression for the grand thermodynamic potential, Eqs. [3.1]–[3.6], is applied to calculate the energy, ΔW, and force, F, of capillary interaction between two spherical particles floating at a fluid interface. ΔW is a superposition of gravity, wetting, and meniscus contributions—see Eqs. [3.9] and [4.7]–[4.9]. For

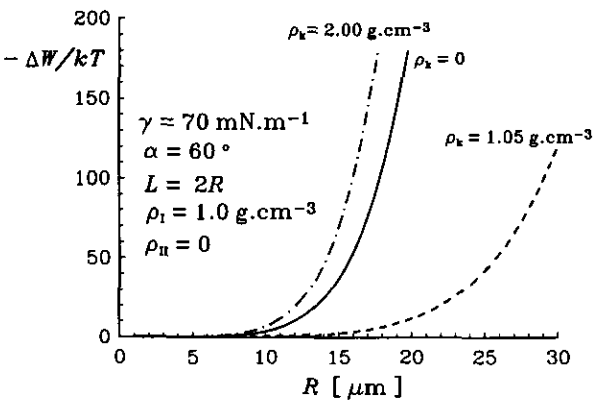

FIG. 11. Dependence of $\Delta W/kT$ on the particle radius, R, for two similar particles for three different values of the particle mass density, ρ_k.

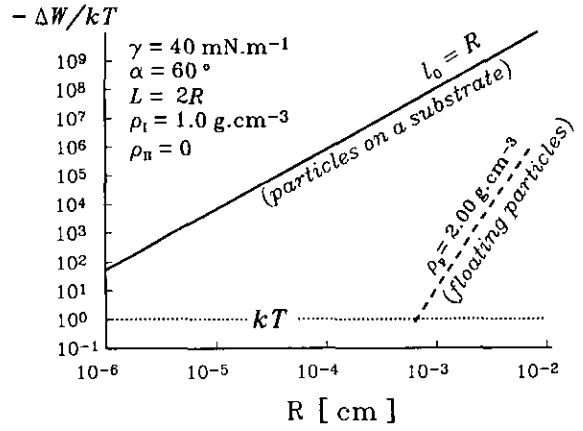

FIG. 12. Plot of $\Delta W/kT$ vs particle radius, R, for two different cases: (i) two particles, floating attached to an air/water interface (the dashed line), and (ii) two particles partially immersed in a liquid layer on a horizontal substrate (the solid line). The last curve (ii) is calculated by means of Eq. [4.11] in Ref. (9).

not-too-small interparticle separations ΔW turns out to be approximately equal to half of the gravitational energy (see Fig. 9), as anticipated previously by Nicholson (6).

(ii) The derived equations allow calculation of ΔW and F not only for large but also for small interparticle separations, in this aspect giving an improvement over the earlier theory by Chan *et al.* (7)—cf. Fig. 2. The results from the energetical approach developed in the present paper and the force approach from Ref. (10) turn out to be in a very good quantitative agreement—see Table 1.

(iii) In some range of interparticle distances the capillary force F obeys a power law, which resembles Newton's law of gravity or Coulomb's law of electricity—see Eq. [6.10] above. In this aspect one can introduce the concept of "capillary charge," Q_1 and Q_2, of the two interacting particles. In particular, depending on whether $Q_1Q_2 > 0$ or $Q_1Q_2 < 0$, the capillary interaction is attractive or repulsive. The range of variation of Q_k ($k = 1, 2$) is determined by Eq. [4.6].

(iv) The capillary interaction energy, ΔW, is a monotonic function of the particle contact angle, α (Fig. 5). However, $|\Delta W|$ exhibits a minimum as a function of the particle density, ρ_k (Fig. 4).

(v) The decrease of the interfacial tension, γ, facilitates the meniscus deformation, thus increasing the magnitude of capillary interaction (Fig. 6).

(vi) In the case of submillimeter particles, considered here, the contribution of the surface tension to the capillary force is much greater than the contribution of the hydrostatic pressure (Fig. 10).

(vii) The capillary interaction between floating particles decreases quickly, with the sixth power of the particle radius, R, when decreasing the particle size—see Eqs. [6.14]–[6.15] and Fig. 11. This is a consequence of the fact that the interaction is brought about by the weight of the particles.

Finally, it should be noted that our results in this paper are subject to the following *restrictions:*

- The expressions for ΔW and F hold for submillimeter particles ($q^2R_k^2 \ll 1$) and for small meniscus slope—cf. Eqs. [5.1] and [5.2]. As shown in Ref. (7) these two conditions are coupled: small particles imply small meniscus slope.
- The assumption that the meniscus surface must be flat and horizontal far from the floating particles is essentially used. Hence the distance between the particles and the wall of the vessel that holds the fluid must be larger than the capillary length q^{-1}—cf. Eq. [4.4]. Otherwise the interaction of the particles with the meniscus near the wall will become important—see e.g., Ref. (11).
- The procedure used in this paper to calculate ΔW and F cannot be applied to the case of particles which are not floating, but are partially immersed in a liquid layer on a substrate. In the latter case the meniscus deformations are due to the capillary rise of the liquid at the particle surfaces, rather than to the particle weight. In particular, Eqs. [6.13] or [7.2] cannot be used to calculate the "capillary charges" Q_1 and Q_2. Instead, one must apply the calculation procedure developed in Refs. (9–11).

APPENDIX: ON THE DERIVATION OF Eq. [6.3]

Some geometrical considerations (cf. Fig. 1) yield

$$b_k = R_k[1 + \cos(\alpha_k + \psi_k)], \quad r_k = R_k\sin(\alpha_k + \psi_k). \quad [A.1]$$

Since the particle radius, R_k, is assumed constant, from Eqs. [A.1] and [5.2] one obtains

$$\frac{db_k}{dL} = -r_k \frac{d\psi_k}{dL}. \quad [A.2]$$

On the other hand, by differentiating Eq. [2.4] one derives

$$\frac{db_k}{dL} = \frac{r_k}{R_k - b_k}\frac{dr_k}{dL}. \quad [A.3]$$

The differentiation of Eq. [4.5] along with Eqs. [A.2] and [A.3] yields

$$\frac{dQ_k}{dL} = \left(\frac{r_k}{b_k - R_k} + \sin\psi_k\right)\frac{dr_k}{dL} = -\frac{db_k}{dL}[1 + O(q^2R_k^2)]. \quad [A.4]$$

In addition, the differentiation of Eq. [7.2] in conjunction with Eq. [2.4] leads to

$$\frac{dQ_k}{dL} = \frac{q^2}{2}\left[r_k^2\frac{db_k}{dL} - 2r_kh_k\frac{dr_k}{dL} - r_k^2\frac{dh_k}{dL}\right]. \quad [A.5]$$

Finally, by substituting from Eqs. [A.3] and [A.4] into Eq. [A.5], one can derive

$$\frac{dQ_k}{dL} = -\frac{1}{2}q^2r_k^2\frac{dh_k}{dL}[1 + O(q^2R_k^2)]. \quad [A.6]$$

A combination of Eqs. [A2], [A4], and [A6] leads to the sought-for eq. [6.3].

ACKNOWLEDGMENTS

This work was supported by the Research and Development Corporation of Japan (JRDC) under the Nagayama Protein Array Project as a part of the program "Exploratory Research for Advanced Technology" (ERATO). Useful discussions with Professor I. B. Ivanov are gratefully acknowledged.

REFERENCES

1. Gerson, D. F., Zaijc, J. E., and Ouchi, M. D., *in* "Chemistry for Energy" (M. Tomlinson, Ed.), ACS Symp. Series, Vol. 90, p. 77. Am. Chem. Soc., Washington D.C., 1979.
2. Henry, J. D., Prudich, M. E., and Vaidyanathan, K. P., *Sep. Purif. Methods* **8,** 81 (1979).
3. Hinsch, K., *J. Colloid Interface Sci.* **92,** 243 (1983).
4. Camoin, C., Roussel, J. F., Fanre, R., and Blanc, R., *Europhys. Lett.* **3,** 449 (1987).
5. Gifford, W. A., and Scriven, L. E., *Chem. Eng. Sci.* **26,** 287 (1971).
6. Nicolson, M. M., *Proc. Cambridge Philos. Soc.* **45,** 288 (1949).
7. Chan, D. Y. C., Henry, J. D., and White, L. R., *J. Colloid Interface Sci.* **79,** 410 (1981).
8. Fortes, M. A., *Can. J. Chem.* **60,** 2889 (1982).
9. Kralchevsky, P. A., Paunov, V. N., Ivanov, I. B., and Nagayama, K., *J. Colloid Interface Sci.* **151,** 79 (1992).
10. Kralchevsky, P. A., Paunov, V. N., Denkov, N. D., Ivanov, I. B., and Nagayama, K., *J. Colloid Interface Sci.* **155,** 420 (1993).
11. Paunov, V. N., Kralchevsky, P. A., Denkov, N. D., Ivanov, I. B., and Nagayama, K., *Colloids Surf.* **67,** 119 (1992).
12. Ivanov, I. B., Kralchevsky, P. A., and Nikolov, A. D., *J. Colloid Interface Sci.* **112,** 97 (1986).
13. Shchukin, E. D., Pertsov, A. V., and Amelina, E. A., "Colloid Chemistry." Moscow Univ. Press, Moscow, 1982. [in Russian]
14. Derjaguin, B. V., *Dokl. Akad. Nauk USSR* **51,** 517 (1946).
15. Jahnke, E., Emde, F., and Lösch, F., "Tables of Higher Functions." McGraw–Hill, New York, 1960.
16. Abramovitz, M., and Stegun, I. A., "Handbook of Mathematical Functions." Dover, New York, 1965.
17. Yoshimura, H., Endo, S., Matsumoto, M., Nagayama, K., and Kagawa, Y., *J. Biochem.* **106,** 958 (1989).
18. Yoshimura, H., Matsumoto, M., Endo, S., and Nagayama, K., *Ultramicroscopy* **32,** 265 (1990).
19. Denkov, N. D., Velev, O. D., Kralchevsky, P. A., Ivanov, I. B., Yoshimura, H., and Nagayama, K., *Langmuir* **8,** 3183 (1992).